



Published in final edited form as:

J Hepatol. 2021 July ; 75(1): 34–45. doi:10.1016/j.jhep.2021.01.043.

Magnesium accumulation upon cyclin M4 silencing activates microsomal triglyceride transfer protein improving NASH

Jorge Simón^{1,2}, Naroa Goikoetxea-Usandizaga¹, Marina Serrano-Maciá¹, David Fernández-Ramos^{1,2,3}, Diego Sáenz de Urturi⁴, Jessica J. Gruskos⁵, Pablo Fernández-Tussy¹, Sofía Lachiondo-Ortega¹, Irene González-Recio¹, Rubén Rodríguez-Agudo¹, Virginia Gutiérrez-de-Juan¹, Begoña Rodríguez-Iruretagoyena¹, Marta Varela-Rey^{1,2}, Paula Gimenez-Mascarell¹, María Mercado-Gomez¹, Beatriz Gómez-Santos⁴, Carmen Fernandez-Rodriguez¹, Fernando Lopitz-Otsoa^{1,3}, Maider Bizkarguenaga^{1,3}, Sibylle Dames⁶, Ute Schaeper⁶, Franz Martin^{7,8}, Guadalupe Sabio⁹, Paula Iruzubieta^{10,11}, Javier Crespo^{10,11}, Patricia Aspichueta^{2,4,12}, Kevan H.-Y. Chu⁵, Daniela Buccella⁵, César Martín¹³, Teresa Cardoso Delgado¹, Luis Alfonso Martínez-Cruz^{1,†}, María Luz Martínez-Chantar^{1,2,*}

¹Liver Disease Laboratory, Center for Cooperative Research in Biosciences (CIC bioGUNE), Basque Research and Technology Alliance (BRTA), Bizkaia Technology Park, Derio, Spain

²Centro de Investigación Biomédica en Red de Enfermedades Hepáticas y Digestivas (CIBERehd), 48160, Bizkaia, Spain

³Precision Medicine and Metabolism Laboratory, Center for Cooperative Research in Biosciences (CIC bioGUNE), Basque Research and Technology Alliance (BRTA), Bizkaia Technology Park, Derio, Spain

⁴Department of Physiology, Faculty of Medicine and Nursing, University of the Basque Country (UPV/EHU), Leioa, Bizkaia, Spain

⁵Department of Chemistry, New York University, New York, NY, USA

⁶Silence Therapeutics GmbH, Berlin, Germany

⁷Centro Andaluz de Biología Molecular y Medicina Regenerativa-CABIMER, Universidad Pablo de Olavide, Universidad de Sevilla, Consejo Superior de Investigaciones Científicas (CSIC), Seville, Spain

This is an open access article under the CC BY-NC-ND license (<http://creativecommons.org/licenses/by-nc-nd/4.0/>).

*Corresponding author. Address: Liver Disease Laboratory, Building 801A, Technologic Park of Biscay, Derio (Biscay), Spain. Tel.: +34-944-061-318; Fax: +34-944-061-301. mlmartinez@cicbiogune.es (M.L. Martínez-Chantar).

†Senior authorship.

Authors' contributions

Conceptualisation: JS, DB, LAM-C, MLM-C. Funding acquisition: JS, FM, PA, DB, TC-D, LAM-C, MLM-C. Investigation: JS, NG-U, MS-M, DF-R, DSdU, JG, PF-T, SL-O, IG-R, RR-A, VG-d-J, BR-I, MV-R, PG-M, MM-G, BG-S, CF-R, FL-O, MB, SD, US, FM, GS, PI, JC, PA, KC, DB, CM, TC-D. Supervision: DB, LAM-C, MLM-C. Writing – original draft, review and editing: JS, US, DB, LAM-C, MLM-C

Conflicts of interest

The authors declare no conflicts of interest related to this submitted work.

Please refer to the accompanying ICMJE disclosure forms for further details.

Supplementary data

Supplementary data to this article can be found online at <https://doi.org/10.1016/j.jhep.2021.01.043>.

⁸Centro de Investigación Biomédica en Red de Diabetes y Enfermedades Metabólicas Asociadas (CIBERDEM), Madrid, Spain

⁹Fundación Centro Nacional de Investigaciones Cardiovasculares Carlos III, Madrid, Spain

¹⁰Gastroenterology and Hepatology Department, Marqués de Valdecilla University Hospital, Santander, Spain

¹¹Clinical and Translational Digestive Research Group, Instituto de Investigación Sanitaria Valdecilla (IDIVAL), Santander, Spain

¹²Biocruces Health Research Institute, Barakaldo, Bizkaia, Spain

¹³Instituto Biofisika (UPV/EHU, CSIC) and Departamento de Bioquímica, Universidad del País Vasco, Bilbao, Spain

Abstract

Background & Aims: Perturbations of intracellular magnesium (Mg^{2+}) homeostasis have implications for cell physiology. The cyclin M family, CNNM, perform key functions in the transport of Mg^{2+} across cell membranes. Herein, we aimed to elucidate the role of CNNM4 in the development of non-alcoholic steatohepatitis (NASH).

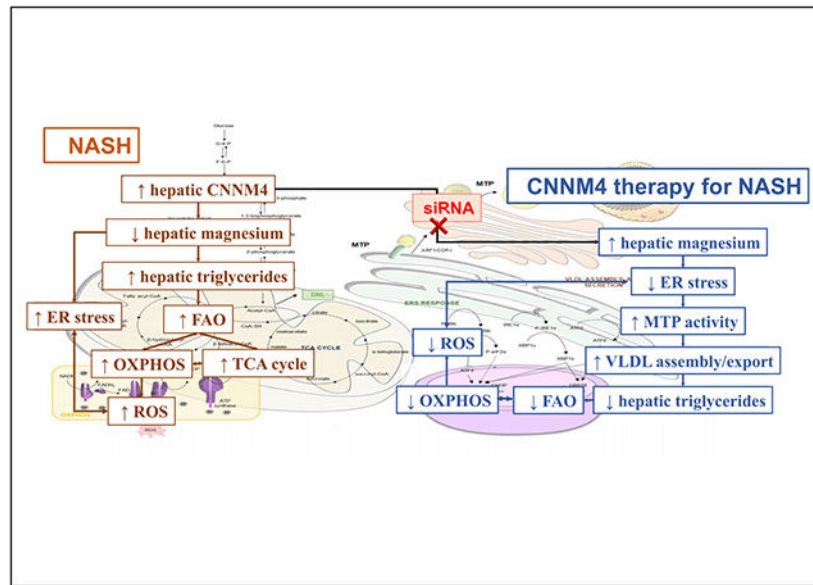
Methods: Serum Mg^{2+} levels and hepatic CNNM4 expression were characterised in clinical samples. Primary hepatocytes were cultured under methionine and choline deprivation. A 0.1% methionine and choline-deficient diet, or a choline-deficient high-fat diet were used to induce NASH in our *in vivo* rodent models. *Cnnm4* was silenced using siRNA, *in vitro* with DharmaFECT and *in vivo* with InvivoFectamine[®] or conjugated to N-acetylgalactosamine.

Results: Patients with NASH showed hepatic CNNM4 overexpression and dysregulated Mg^{2+} levels in the serum. *Cnnm4* silencing ameliorated hepatic lipid accumulation, inflammation and fibrosis in the rodent NASH models. Mechanistically, CNNM4 knockdown in hepatocytes induced cellular Mg^{2+} accumulation, reduced endoplasmic reticulum stress, and increased microsomal triglyceride transfer activity, which promoted hepatic lipid clearance by increasing the secretion of VLDLs.

Conclusions: CNNM4 is overexpressed in patients with NASH and is responsible for dysregulated Mg^{2+} transport. Hepatic CNNM4 is a promising therapeutic target for the treatment of NASH.

Lay summary: Cyclin M4 (CNNM4) is overexpressed in non-alcoholic steatohepatitis (NASH) and promotes the export of magnesium from the liver. The liver-specific silencing of *Cnnm4* ameliorates NASH by reducing endoplasmic reticulum stress and promoting the activity of microsomal triglyceride transfer protein.

Graphical Abstract



Keywords

Non-alcoholic steatohepatitis; NASH; Cyclin M4; CNNM4; Magnesium; Therapy; siRNA; Endoplasmic reticulum stress; Microsomal triglyceride transfer protein; MTP

Introduction

Dietary imbalances, such as a low intake of magnesium, are recognised as the root cause of diseases. Although daily magnesium recommended intake is 300–400 mg/day, there is a growing concern about decreased intake in last decade, attributable to changes in dietary habits and food processing.^{1,2} Its ionic form, Mg^{2+} , is the most abundant divalent cation in the cell and it is required as a cofactor for over 300 enzymatic reactions.³ An intricate network of Mg^{2+} transporters participate in its uptake and excretion, allowing its flux across cellular membranes, thus impacting Mg^{2+} homeostasis and distribution.¹

Mg^{2+} supplementation reduces mortality from hepatic complications arising from alcohol intake or steatosis.⁴ Hypomagnesaemia is present in several comorbidities of non-alcoholic fatty liver disease (NAFLD) such as insulin resistance and type 2 diabetes,⁵ cardiovascular complications,⁶ and obesity.⁷ Moreover, deficiencies in Mg^{2+} are related to inflammatory responses, mitochondrial dysfunction, and decreased activity of the antioxidant system, all features of liver diseases.⁸

The term NAFLD encompasses a group of pathologies characterised by chronicity with serial progression from steatosis to non-alcoholic steatohepatitis (NASH) and cirrhosis.⁹ Such progression is mediated by the increased production of reactive oxygen species (ROS), lipotoxicity, mitochondrial dysfunction, and the development of endoplasmic reticulum (ER) stress.¹⁰ Remarkably, ER stress has been proposed to be an important mechanism because it disrupts calcium (Ca^{2+}) transport through ATPases¹¹ and leads to protein misfolding.¹² It

has been widely characterised in both NAFLD and NASH patients, together with impaired VLDL assembly and secretion.^{13,14}

NAFLD is a global health problem with an estimated prevalence of around 25% among the adult population, being expected to increase.⁹ Changes in lifestyle habits are the most common recommendations for the clinical management of NAFLD, but it is difficult to achieve the long-term compliance of patients, making pharmacological alternatives attractive.

Among the various magnesiotropic proteins, the cyclin M (CNNM) family and their Bateman-module-mediated interactions with phosphatases of regenerating liver (PRLs) are of particular interest.¹⁵ PRLs are implicated in tumour progression and metastasis,^{16,17} including liver cancer, with Mg²⁺ perturbations reported in such.¹⁸ Although the CNNMs emerged as interacting molecular partners of PRLs,¹⁷ a new perspective proposes targeting CNNMs to modulate Mg²⁺ homeostasis more specifically.¹⁹ The functions of hepatic CNNMs in this regard are unknown, and their significance as pharmacological targets remains underexplored.

In the present study, we demonstrated the relevance of the differential expression of CNNM4 in NASH development, showing its functional role in transporting hepatic Mg²⁺. Moreover, we identified CNNM4 as a potential target for NASH treatment.

Patients and methods

Patients

Measurements of serum Mg²⁺ and hepatic *CNNM1-4* mRNA, and immunohistochemical CNNM4 analysis were performed in different cohorts recruited at the Hospital Marqués de Valdecilla, Santander, Spain (Fig. S1A and B).

Animal maintenance and preclinical studies

Mice were maintained with *ad libitum* access to water and a choline-deficient diet with 0.1% methionine (0.1% MCDD) or a choline-deficient, high-fat diet (CD-HFD). A control group was maintained on a regular diet (SC diet).

Treatment of primary mouse hepatocytes and THLE-2 cells

Upon attachment, isolated mouse primary hepatocytes were transfected by overnight incubation with siRNA using DharmaFECT 1 or a CNNM4 expression plasmid using jetPRIME®. Cells were maintained and incubated for an additional 24 h under different conditions.

Cnnm4 silencing *in vivo*

Mice fed a 0.1% MCDD for 2 weeks or a CD-HFD for 3 weeks were repeatedly administered an siRNA using InvivoFectamine® 3.0 Reagent through tail vein injection. Mice were sacrificed after 4 weeks on 0.1% MCDD and 6 weeks on CD-HFD, respectively. For *Cnnm4* GalNAc-siRNA delivery, mice fed for 3 weeks on 0.1% MCDD were treated

once, subcutaneously, and sacrificed after a total of 6 weeks on the diet. Samples of liver, white adipose tissue (WAT), and serum were collected.

Statistical analysis

All the experiments were performed at least in triplicate, with $n = 3$ (*in vitro*) and $n = 4$ (*in vivo*). The data are expressed as mean \pm SEM and represent the fold change *vs.* control mean value when indicated. Statistical significance was determined using Prism 8 (GraphPad Software, San Diego, CA, USA). Groups were compared by 1-way analysis of variance (ANOVA) followed by *post hoc* Bonferroni tests (for 3 or more groups) or the Student *t* test (for 2 groups).

Results

CNNM4 is overexpressed in clinical and preclinical NASH

To investigate Mg^{2+} dysregulation in NASH, we determined Mg^{2+} levels in sera from a cohort of 50 age- and BMI-matched patients (Fig. S1A), observing increased levels of the cation in NASH patients (Fig. 1A). Mg^{2+} levels did not correlate with other NASH biomarkers (data not shown).

Considering the magnesiotropic role of the CNNM family,¹⁹ we sought to assess whether dysregulated *CNNM* expression could be the cause of the elevated serum Mg^{2+} . The hepatic mRNA levels of each *CNNM* were assessed in another cohort of 40 patients (Fig. S1B), showing a significant overexpression of *CNNM1* and *CNNM4* in NASH patients (Fig. 1B). In addition, an increase in *Cnnm4* mRNA expression was observed in primary hepatocytes treated with methionine and choline-deficient (MCD) medium (Fig. 1C), an *in vitro* model that displays features of NASH such as ROS overproduction and lipid accumulation.^{20,21}

Similarly, hepatic CNNM4 overexpression in NASH was confirmed by immunohistochemical protein determination in clinical samples (Fig. 1D) and animal models – mice fed a 0.1% MCDD (Fig. 1E) and CD-HFD (Fig. 1F). These animal models also showed elevated *Cnnm4* mRNA, as did primary hepatocytes (Fig. S1C and D). By contrast, *Cnnm1* overexpression was observed in neither the *in vitro* nor *in vivo* NASH models. To evaluate protein stability, human THLE-2 cells were treated with MLN4924 to inhibit NEDDylation, which prevents proteasome-mediated degradation,²² resulting in decreased CNNM4 expression (Fig. S1E). The expression of other Mg^{2+} transporters was determined in animal models (Fig. S1F) and clinical samples (Fig. S1G), showing that CNNM4 is unique among Mg^{2+} transporters in its upregulation in all conditions.

Targeting CNNM4 ameliorates NASH

The possible role of CNNM4 in NASH development was examined by *in vitro* screening by specifically silencing each *Cnnm* in primary hepatocytes using small interfering RNA (siRNA). Targeting *Cnnm4* (si*Cnnm4*) alone effectively reduced MCD-induced lipid accumulation (Fig. 2A). The expression of each *Cnnm* and *Prl* mRNA was evaluated, confirming the specific and effective silencing of *Cnnm* (Fig. S2A) and eliminating the

possibility of *Pr1* regulation when targeting *Cnnm4* (Fig. S2B). Additionally, *CNNM4* silencing in THLE-2 cells also reduced MCD-induced lipid accumulation (Fig. S2C and D).

Taking into consideration the *CNNM4* overexpression observed in NASH, and the si*Cnnm4*-derived reduction of lipid accumulation, the therapeutic potential of silencing *Cnnm4 in vivo* was explored. Mice were fed a 0.1% MCDD to induce steatosis development, increased oxidative stress, inflammation, and fibrosis in a short period of time.²³ At 2 weeks, by which steatosis²¹ and *CNNM4* overexpression are observable (Fig. 1E), 0.1% MCDD-fed mice were separated into 2 groups and treated repeatedly with either an siRNA against *Cnnm4* (0.1% MCDD + si*Cnnm4*) or an unrelated control (0.1% MCDD + siCtrl), using InvivoFectamine 3.0®. The mice were sacrificed at the fourth week. Interestingly, the mice fed the 0.1% MCDD showed hepatic *CNNM4* overexpression, whereas *Cnnm4* silencing reduced diet-induced steatosis (Fig. 2B and Fig. S2E). Alpha-smooth muscle actin (α SMA) staining revealed that fibrosis, another NASH hallmark, was induced by 0.1% MCDD and attenuated by si*Cnnm4* (Fig. S2F). Furthermore, the treatment also reduced serum alanine aminotransferase (ALT) levels, a marker of liver damage (Fig. S2G).

In a different NASH murine model, mice were fed a CD-HFD, as this leads to a pattern of pathology more similar to that observed in humans.²⁴ Although studies using this model tend to be performed for longer than 6 weeks,²⁴ our group previously showed that mice developed early NASH phenotypes comprising weight gain, steatosis, and inflammation as early as this point in time.²¹ After 3 weeks on the diet, at which point *CNNM4* was already overexpressed (Fig. 1F), the CD-HFD-fed group was divided and treated with si*Cnnm4* (CD-HFD + si*Cnnm4*) or siCtrl (CD-HFD + siCtrl). They were sacrificed after 6 weeks and, similarly to in the previous results, the mice fed the CD-HFD showed hepatic *CNNM4* overexpression, while the siRNA therapy reduced steatosis (Fig. 2C and Fig. S2H) and fibrosis development (Fig. S2I). Serum ALT levels remained unaltered (Fig. S2J).

CNNM4 acts in the liver as a magnesium exporter

Despite the magnesiotropic role of *CNNM4* in kidney epithelia,²⁵ its physiological function in the liver remains largely unknown. The possible relationship between increased serum Mg^{2+} levels and hepatic *CNNM4* overexpression (Fig. 1A and D) led us to anticipate a modulation of the cation in the studied NASH animal models. The measurement of Mg^{2+} in the serum revealed an increase in CD-HFD-fed mice and a decrease under si*Cnnm4* treatment in both the CD-HFD and 0.1% MCDD models (Fig. 3A).

To confirm the hypothesis of *CNNM4* being a hepatic Mg^{2+} exporter, *CNNM4*-related Mg^{2+} flux in hepatocytes was assessed *in vitro*. Fluorescent staining with the ratiometric probe MagS was used to estimate the relative levels of cytosolic free Mg^{2+} in live cells treated with si*Cnnm4*. MagS is an analogue of Mag-FURA-2, developed by the Buccella group,²⁶ which displays similar metal recognition but enhanced optical properties. Furthermore, taking into consideration the key role of mitochondria in hepatocyte function,^{27,28} we sought to explore the mitochondrial Mg^{2+} levels in the aforementioned si*Cnnm4* conditions. For this purpose, we developed MagS-TPP, a targeted variant functionalised with a phosphonium group for delivery to the mitochondrial matrix (Fig. 3B). The new dye exhibits a selectivity profile

similar to MagS and binds to Mg^{2+} with an apparent dissociation constant suitable for the detection of typical intracellular concentrations of free Mg^{2+} (Fig. S3).

Mitochondrion- and non-targeted fluorescent indicators were applied, revealing an increase in both cytosolic and mitochondrial free Mg^{2+} levels in cells with reduced *Cnnm4* expression (Fig 3C), combined with a decrease in the cation in the extracellular medium (Fig 3D). The silencing of other *Cnnm* family members did not lead to significant alterations in intra- or extracellular Mg^{2+} (Fig. 3E and F), thus eliminating their possible contribution to Mg^{2+} homeostasis in the hepatocyte. These results support the notion that the observed decrease in serum Mg^{2+} of mice treated with si*Cnnm4* could be a consequence of its accumulation in the liver (Fig. 3G).

CNNM4-mediated magnesium accumulation reduces lipid content

The association between CNNM4 and magnesium efflux prompted us to characterise the contribution of Mg^{2+} homeostasis to NASH development. The relative content of the cation in primary hepatocytes under MCD conditions was determined, showing an MCD-induced decrease in Mg^{2+} and an increase upon silencing *Cnnm4* (Fig. 4A). Taking the latter into consideration, a possible inverse relationship between hepatic Mg^{2+} and lipid content was investigated. Magnesium depletion in the cell medium (0 mM Mg^{2+}) resulted in an increased hepatocyte lipid content, while silencing *Cnnm4* reduced this effect (Fig. 4B). In line with the results of a clinical trial addressing the beneficial properties of magnesium,⁴ Mg^{2+} supplementation (5 mM Mg^{2+}) reverted MCD-induced lipid accumulation in hepatocytes without effects under normal conditions (1 mM Mg^{2+}) (Fig. S4A). Neither Mg^{2+} depletion nor supplementation affected *Cnnm4* expression (data not shown).

To eliminate the possibility of other Mg^{2+} transporters contributing to si*Cnnm4*-induced lipid reduction, their expression was characterised under various conditions. We observed an increase in the expression of *Transient Receptor Protein Melastatin 6* (*Trpm6*) (Fig. S4B), suggesting that the lipid reduction may also be the result of increased Mg^{2+} entry. As there is no commercial inhibitor for TRPM6, its isoform 7 was inhibited with 2-aminoethyl diphenyl borinate (2-APB)²⁹ to further investigate the contribution of Mg^{2+} entry. We observed that the lipid accumulation induced by inhibiting Mg^{2+} import was normalised by si*Cnnm4* (Fig. S4C). Finally, the functional relationship between cellular Mg^{2+} levels and steatosis was investigated by overexpressing CNNM4 via transient transfection, which reduced Mg^{2+} levels (Fig. 4C and D) and raised lipid contents in hepatocytes (Fig. 4E). Remarkably, Mg^{2+} supplementation did not attenuate CNNM4-induced lipid accumulation (Fig. 4D and E).

Endoplasmic reticulum and oxidative stress are reduced by silencing cyclin M4

Considering that ROS production and inflammation are major drivers of NASH progression,^{10,28} mitochondrial ROS were assessed in primary hepatocytes, showing a reduction in MCD-induced ROS production upon silencing *Cnnm4* (Fig. 5A). The development of ER stress is also considered a 'second hit', linked to oxidative stress³⁰ and with an existing Mg^{2+} flux between the ER and mitochondria.³¹ Thus, we hypothesised that ER integrity might be affected by CNNM4-induced Mg^{2+} fluctuations in NASH. Therefore, cytosolic calcium (Ca^{2+}), an ER-stress indicator, was quantified in primary hepatocytes. The increased

[Ca²⁺]_{cytosol} observed under MCD stimulation and siRNA-derived attenuation (Fig. 5B), together with the partial co-localisation of Mg²⁺ and ER (Fig. S5A), suggested a protective effect of silencing *Cnnm4*, not only for mitochondria, but also for the ER. This was further addressed by characterising the release of Ca²⁺ from the ER by stimulating primary hepatocytes with ATP, reported to promote the P2Y receptor-mediated release of Ca²⁺ into the cytosol.³² Interestingly, an MCD-induced decreased capacity and then normalisation upon silencing *Cnnm4* were observed (Fig. 5C), while ER labelling was decreased under the MCD and recovered by *Cnnm4* siRNA (Fig. 5D). The relationship between ER stress and hepatic lipid content was elucidated by treating primary hepatocytes with tunicamycin, an ER-stress inducer.³³ A dose-dependent lipid accumulation was observed after 24 h of treatment, while si*Cnnm4* led to a decrease in lipid content (Fig. 5E and Fig. S5B).

When characterising ROS production *in vivo*, si*Cnnm4*-treated mice showed reduced dihydroethidium (DHE) staining (Fig. 5F), probably as a result of the oxidative activity measured by various pathways (Fig. S5C–F). Although oxidative stress was not determined in the study with CD-HFD mice, the observed reduction in fatty acid oxidation (Fig. S5G) is consistent with a ROS reduction. The regulation of the oxidative stress response prompted us to evaluate ER stress in the *in vivo* models of NASH using different markers,³⁴ demonstrating upregulation in both NASH models and reduction under si*Cnnm4*, suggesting that the latter diminished the ER-stress response (Fig. 5G and Fig. S5G). ER-stress associated signalling pathways were also evaluated, showing a decreased activation of S6 ribosomal protein (S6) by phosphorylation.³⁵

CNNM4 inhibition increases MTP activity, promoting VLDL secretion

The formation of pre-VLDL, the first step of VLDL assembly, takes place in the ER.³⁶ During this step, a small number of triglycerides (TGs) are associated with an apolipoprotein B (APOB) molecule and embedded in a phospholipid monolayer by the microsomal triglyceride transfer protein (MTP).³⁶ The alterations of ER integrity previously observed under MCD and the reversion of such by si*Cnnm4* suggested a possible modulation of MTP activity. Remarkably, the protein was increased upon silencing *Cnnm4* in both the primary hepatocytes (Fig. 6A) and *in vivo* rodent NASH models (Fig. 6B).

The serum TGs of mice fed a 0.1% MCDD were found to decrease, owing to intrahepatic lipid accumulation, and were partially restored by *Cnnm4* siRNA (Fig. S6A), suggesting an improved VLDL secretion. Therefore, we determined the relative APOB100 concentrations in the serum, an indicator of circulating lipoprotein particles, observing an increase under si*Cnnm4* conditions (Fig. 6C and Fig. S6B). The contribution of increased lipid secretion mediated by VLDL was further confirmed by measuring APOB100 in serum extracted directly from the cava vein, with VLDLs as the main component, showing an increased APOB100 content (Fig. S6C). The hepatic TG secretion rate, as well as the VLDL content, were determined after administering poloxamer P407 to inhibit lipoprotein lipase.³⁷ Remarkably, both the secretion rate and the VLDL lipid content tended to increase upon silencing *Cnnm4* (Fig. 6D and Fig. S6D). MTP was then inhibited in primary hepatocytes by 24-h lomitapide incubation, a selective inhibitor,³⁸ or with a specific siRNA (si*Mtp*). As

expected, the lipid reduction observed upon CNNM4 knockdown was absent under lomitapide stimulation (Fig. 6E) or *Mtp* silencing conditions (Fig. 6F and Fig S6E).

The possible atherogenic secondary effects are a concern when it comes to promoting VLDL secretion. Furthermore, when determining the Mg^{2+} content in isolated VLDL, the observed restoration in the group treated with the *Cnnm4* siRNA (Fig. S7A) suggested a possible impact on the WAT. The measurement of the relative fatty acid oxidation (FAO) capacity of WAT revealed a tendency to increase with the siRNA treatment (Fig. S7B), together with an increased expression of genes involved in lipid oxidation, mitochondrial biogenesis, and thermogenesis (Fig. S7C). This result was corroborated in primary WAT adipocytes, where Mg^{2+} supplementation increased glycerol production, an indicator of lipolysis without subsequent non-esterified fatty acid (NEFA) production (Fig. S7D). The same result was observed with conditioned medium obtained from primary hepatocytes cultured under MCD and si*Cnnm4* conditions (Fig. S7E).

The siRNA conjugation with GalNAc offers a potential therapy

Considerable progress has recently been made in the development of oligonucleotide-based therapeutics, whereby the silencing of target genes is being explored in clinical studies.³⁹ To transfer the presented discoveries into a therapeutic approach suitable for clinical development, a newly identified *Cnnm4* siRNA candidate was conjugated to an N-acetylgalactosamine (GalNAc) cluster that binds to the asialo-glycoprotein receptors predominantly expressed in hepatocytes. This technology offers a potentially safe, specific, and efficient mode of delivery for targeting therapeutic molecules to hepatocytes.⁴⁰

The specific inhibition of *Cnnm4* was achieved in primary hepatocytes through receptor-mediated uptake by adding different doses of a GalNAc-conjugated siRNA against *Cnnm4* (GalNAc siRNA) directly to the culture medium (Fig. 7A). The lipid accumulation induced by MCD medium was reduced by the GalNAc siRNA treatment (Fig. 7B), and Mg^{2+} accumulation in hepatocytes was observed indirectly through its decrease in the extracellular medium (Fig. 7C). ROS overproduction upon MCD stimulation was also reduced by treating the hepatocytes with the conjugate (Fig. 7D).

Finally, the effectiveness of *Cnnm4* GalNAc siRNA was evaluated *in vivo* in mice fed a 0.1% MCDD for 6 weeks, leading to a more severe NASH phenotype.²¹ The treatment was initiated at the 3-week point with a single injection of different doses (1 or 5 mg/kg) of *Cnnm4* GalNAc siRNA (0.1% MCDD + GalNAc siRNA) or a control siRNA conjugate (0.1% MCDD + siCtrl). A specific and significant inhibition of *Cnnm4* mRNA expression was detected in mice administered either 1 or 5 mg/kg (Fig. 7E), while the Mg^{2+} levels in serum were reduced in line with a presumed hepatic Mg^{2+} accumulation (Fig. 7F). Importantly, CNNM4 inhibition by GalNAc siRNA significantly reduced hepatic lipid accumulation and alleviated the inflammatory response and fibrosis development (Fig. 7G).

Discussion

The studies described herein pinpoint CNNM4 as a key regulator of Mg^{2+} homeostasis in hepatocytes and a potential therapeutic target for NASH. To date, research performed on this

cation in liver pathologies has shown a protective effect of Mg^{2+} supplementation⁴ and revealed Mg^{2+} deficiencies in patients with cirrhosis or liver cancer.¹⁸ Indeed, hypomagnesaemia is frequently observed in NASH comorbidities.^{6,7} However, there is still a dearth of knowledge on the implications of Mg^{2+} perturbations for the development of NASH, and nothing has been reported about magnesiotropic proteins and their modulation in the liver.

Previous studies have mainly focused on PRL, the interacting partner of CNNM, associating its expression with poor prognosis in multiple cancer types including liver,^{16,17} whereas studies of CNNMs have been limited to their role in transporting Mg^{2+} across epithelia.²⁵ Herein, we demonstrate that CNNM4 is a contributor to NASH, as it is overexpressed in preclinical models and clinical samples of the pathology. The reduction in CNNM4 expression in THLE-2 cells upon inhibiting NEDDylation suggests the involvement of post-translational mechanisms in the modulation of the stability of CNNM4 during NASH. This is further confirmed by the reduction of MCD-induced lipid accumulation by the specific silencing of *Cnnm4*, which does not happen upon silencing other *Cnnms*. Regarding the effect of targeting *Cnnm4* on NASH development, preclinical studies in rodent models showed promising effects of an siRNA-based therapy in mice fed either a 0.1% MCDD or CD-HFD. Significantly, both diets increase lipid accumulation and fibrosis development, but the siRNA therapy ameliorates both hallmarks of the disease. The role that CNNM4 may play in other cell populations such as hepatic stellate cells requires more research, as do the possible post-transcriptional and post-translational mechanisms that may contribute to CNNM4 overexpression.

The role of the hepatocyte in NASH and its subsequent progression has been widely characterised.^{27,28} The silencing of *Cnnm4* may reduce oxidative activity, leading to reduced oxidative stress, which could contribute to a reduction in fibrosis development. Although the development of oxidative stress was not characterised in the CD-HFD *in vivo* study, the observed reduction in FAO and lipid contents prompts to expect a similar reduction. The relevance of the hepatocyte in NASH progression and the implications of modulating CNNM4 were further characterised in mice fed a 0.1% MCDD for 6 weeks. Herein, we also demonstrated that targeting CNNM4 ameliorated NASH, even that with a more severe phenotype.²¹ To develop a possible therapeutic approach, an siRNA was conjugated with GalNAc allowing stable and liver-specific delivery,⁴⁰ with results similar to those observed when targeting *Cnnm4* with the liposomal siRNA formulation after 4 weeks on the 0.1% MCDD.

Although CNNM4 has been characterised as a Mg^{2+} transporter in kidney epithelia,⁴¹ the CNNM4-mediated flux of the cation in the liver remains unknown. Our research shows CNNM4 to be a Mg^{2+} exporter in the hepatocyte, as its specific silencing increases intracellular Mg^{2+} . Hepatic si*Cnnm4*-induced Mg^{2+} accumulation was characterised in all the preclinical studies through the quantification of the cation in serum, currently the only feasible method because of the lack of available tools for directly measuring hepatic Mg^{2+} *in vivo*. CNNM4 overexpression in the clinical samples correlated with the increased Mg^{2+} serum levels observed. The possible contribution of other, non-liver-related factors was eliminated by the BMI and age pairing of the samples. Similarly to clinical NASH, increased

serum levels of the cation were observed in mice fed a CD-HFD, whereas in the 0.1% MCDD model, the lower Mg^{2+} content in the diet may have masked the expected CNNM4-induced increase in serum. The possible involvement of Mg^{2+} content in NASH-inducing diets might be a topic of interest for future research.

The finding that hepatocyte Mg^{2+} content is inversely correlated with lipid accumulation also suggests a possible role of the cation in NASH. Decreases in intracellular Mg^{2+} , whether induced by MCD stimulation or transfection with the CNNM4 vector, were accompanied by increased lipid accumulation. Accordingly, Mg^{2+} -depleted culture medium also increased hepatocyte lipid content. Remarkably, the action of CNNM4 in modulating Mg^{2+} homeostasis prevails over that of other transporters, as the inhibition of Mg^{2+} import with 2-APB²⁹ leads to an expected lipid accumulation, which is reverted under si*Cnnm4* treatment. Mg^{2+} supplementation decreases hepatocyte lipid content under MCD stimulation, whereas under vector-induced CNNM4 overexpression, such supplementation is not sufficient to counteract the increase. These observations suggest the relevance of not only adequate Mg^{2+} intake, but also the correct balance of the proteins implicated in its homeostasis, such as CNNM4.^{1,2}

Combined with oxidative stress, ER stress has been characterised as an additional driver of NASH progression,^{10,14} with a demonstrated connection between these 2 'hits'.³⁰ In our study, the characterised MCD-induced development of ER stress was reversed by silencing *Cnnm4*. Despite the current lack of effective methods for determining the Mg^{2+} content in the ER, the partial co-location observed and the recently characterised Mg^{2+} flux between the ER and mitochondria³¹ suggest that the induced Mg^{2+} accumulation somehow protects the hepatocyte from ER-stress development. Likewise, the development of ER stress by hepatocytes upon tunicamycin stimulation induces lipid accumulation in a dose-dependent manner, and si*Cnnm4* reduced this effect. *In vivo*, the ER stress response was shown to increase under NASH development and be attenuated upon silencing *Cnnm4*, a phenomenon involving the phosphorylation-mediated activation of S6 and independent of other pathways such as AMP-dependent protein kinase or extracellular signal-related protein kinase 1/2.

The reduction of ER stress under *Cnnm4* knockdown might be the cause of the increased MTP activity observed. The MTP is located in the ER and catalyses the first step of pre-VLDL formation and transfer to the Golgi for its maturation,³⁶ whereas APOB100 is co-translationally expressed while MTP is functioning.⁴² Thus, increased MTP activity is accompanied by increased APOB100 in the serum. These findings, together with the restoration of TGs in the serum of treated 0.1% MCDD-fed mice and lipid content in secreted VLDLs, suggest that *Cnnm4* knockdown may increase MTP activity in a direct or indirect manner and, consequently, promote VLDL secretion from the liver. This is further supported by the observation that MTP inhibition in hepatocytes blocked the reduction of lipid accumulation by *Cnnm4* siRNA treatment. The possible implications of other pathways involved in lipid resolution and the Mg^{2+} -induced changes in metabolic pathways require further investigation.

Interestingly, secondary atherogenic effects from targeting *Cnnm4* are not expected as TGs are restored to normal levels rather than above. Moreover, the hepatic Mg^{2+} accumulation

leads to the restoration of the cation in secreted VLDLs, which may promote their catabolism by WAT, as the cation acts as a cofactor in reactions involving ATP.³ Thus, Mg²⁺ restoration may promote the lipolytic and FAO activities of WAT, as the increase in glycerol production upon stimulating primary adipocytes with Mg²⁺ or conditioned medium from primary hepatocytes is not accompanied by increased NEFA production. Indeed, the expression in the WAT of several genes involved in lipid catabolism increased in the group of mice treated with the *Cnnm4* siRNA. Although the effect of CNNM4 on the oxidative activity of WAT needs to be investigated more deeply, the present study points out a possible anti-atherogenic effect of silencing *Cnnm4*.

In summary, CNNM4 appears to be a feasible candidate for developing therapies against NASH. CNNM4-based therapy induces hepatic Mg²⁺ and, consequently, reduces steatosis and other hallmarks of the disease such as oxidative or ER stress, while reducing fibrosis. Additionally, ER recovery might lead to increased MTP activity, promoting VLDL formation, increasing hepatic lipid export, and reducing lipid accumulation (see the Graphical Abstract). Furthermore, the possibility of conjugating the siRNA with a GalNAc molecule and the observed effectiveness in ameliorating NASH, even that of a severe phenotype, points to CNNM4 as an attractive hepatocyte target for treatment.

Supplementary Material

Refer to Web version on PubMed Central for supplementary material.

Acknowledgments

Financial support

Ministerio de Ciencia e Innovación, Programa Retos-Colaboración RTC2019-007125-1 (for JS and MLM-C); Instituto de Salud Carlos III, Proyectos de Investigación en Salud DTS20/00138 (for JS and MLM-C); Departamento de Industria del Gobierno Vasco (for MLM-C); Ministerio de Ciencia, Innovación y Universidades MICINN: SAF2017-87301-R and RTI2018-096759-A-100 integrado en el Plan Estatal de Investigación Científica y Técnica y Innovación, cofinanciado con Fondos FEDER (for MLM-C and TCD, respectively); BIOEF (Basque Foundation for Innovation and Health Research); EITB Maratoia BIO15/CA/014; Asociación Española contra el Cáncer (MLM-C, TCD); Fundación Científica de la Asociación Española Contra el Cáncer (AECC Scientific Foundation) Rare Tumor Calls 2017 (for MLM); La Caixa Foundation Program (for MLM); Fundación BBVA UMBRELLA project (for MLM); BFU2015-70067-REDC, BFU2016-77408-R, and BES-2017-080435 (MINECO / FEDER, UE) and the FIGHT-CNNM2 project from the EJP RD Joint Transnational Call (JTC2019) (Ref. AC19/00073) (for LAM-C); RTI2018-095134-B-100 and Grupos de Investigación del Sistema Universitario Vasco (IT971-16) (for PA); National Institutes of Health under grant CA217817 (for DB); AGL2014-54585-R, AGL-2017-86927-R and EQC2018-004897-P from MINECO; PC0148-2016-0149 and PAI-BIO311 from Junta de Andalucía (for FM). Ciberehd_ISCIII_MINECO is funded by the Instituto de Salud Carlos III. We thank Silence Therapeutics plc. for the financial support provided. We thank MINECO for the Severo Ochoa Excellence Accreditation to CIC bioGUNE (SEV-2016-0644).

Data availability statement

The data that support the findings of this study are available from the corresponding author, M.L.M.-C. upon reasonable request.

Abbreviations

0.1% MCDD choline-deficient diet with 0.1% methionine

2-APB	2-aminoethyl diphenyl borinate
αSMA	alpha-smooth muscle actin
ALT	alanine aminotransferase
AMPK	AMP-dependent protein kinase
APOB	apolipoprotein B
BIP/GRP78	binding immunoglobulin protein
CD-HFD	choline-deficient, high-fat diet
CNNM4	cyclin M4
CNNM	cyclin M family
DHE	dihydroethidium
eIF2α	(eukaryotic initiation factor 2α)
ER	endoplasmic reticulum
ERK 1/2	extracellular signal-related protein kinase 1/2
FAO	fatty acid oxidation
MagS	magnesium-specific
MagS-TPP	mitochondrion-targeted magnesium-specific
MCD	methionine and choline-deficient
MTP	microsomal triglyceride transfer protein
NAFLD	non-alcoholic fatty liver disease
NASH	non-alcoholic steatohepatitis
NEFA	non-esterified fatty acid
GalNAc	N-acetylgalactosamine
PRLs	phosphatases of regenerating liver
ROS	reactive oxygen species
S6	S6 ribosomal protein
SC diet	regular diet
siRNA	small interfering RNA
Trpm6	transient receptor protein melastatin 6
TGs	triacylglycerides

WAT	white adipose tissue
XBPIs	x-box binding protein 1 isoform s

References

- [1]. Jannen-dechent W, Ketteler M. Magnesium basics. *Clin Kidney J* 2012;5:i3–i14. [PubMed: 26069819]
- [2]. Razzaque MS. Magnesium: are we consuming enough? *Nutrients* 2018;10:1863.
- [3]. De Baaij JHF, Hoenderop JGJ, Bindels RJM. Magnesium in man: implications for health and disease. *Physiol Rev* 2015;1920:1–46.
- [4]. Wu L, Zhu X, Fan L, Kabagambe EK, Song Y, Tao M, et al. Magnesium intake and mortality due to liver diseases: results from the third national health and nutrition examination survey cohort. *Sci Rep* 2017;7:17913. [PubMed: 29263344]
- [5]. Barbagallo M, Di Bella G, Brucato V, D'Angelo D, Damiani P, Monteverde A, et al. Serum ionized magnesium in diabetic older persons. *Metabolism* 2014;63:502–509. [PubMed: 24462317]
- [6]. Rosique-Esteban N, Guasch-Ferré M, Hernández-Alonso P, Salas-Salvadó J. Dietary magnesium and cardiovascular disease: a review with emphasis in epidemiological studies. *Nutrients* 2018;10:168.
- [7]. Gonzalez L, Rodri H, Rodri M. Hypomagnesemia, insulin resistance, and non-alcoholic steatohepatitis in obese subjects. *Arch Med Res* 2005;36:362–366. [PubMed: 15950075]
- [8]. Casas-Grajales S, Muriel P. Antioxidants in liver health. *World J Gastro-intest Pharmacol Ther* 2015;6:59–72.
- [9]. Younossi ZM, Koenig AB, Abdelatif D, Fazel Y, Henry L, Wymer M. Global epidemiology of nonalcoholic fatty liver disease – meta-analytic assessment of prevalence, incidence, and outcomes. *Hepatology* 2016;64:73–84. [PubMed: 26707365]
- [10]. Sanyal AJ. Mechanisms of disease: pathogenesis of nonalcoholic fatty liver disease. *Nat Clin Pract Gastroenterol Hepatol* 2005;2:46–53. [PubMed: 16265100]
- [11]. Meldolesi J, Pozzan T. The endoplasmic reticulum Ca²⁺ store: a view from the lumen. *Trends Biochem Sci* 1998;23:10–14. [PubMed: 9478128]
- [12]. Schroder M, Kaufman RJ. ER stress and the unfolded protein response. *Mutat Res* 2005;569:29–63. [PubMed: 15603751]
- [13]. Gregor MF, Yang L, Fabbrini E, Mohammed BS, Eagon JC, Hotamisligil GS, et al. Endoplasmic reticulum stress is reduced in tissues of obese subjects after weight loss. *Diabetes* 2009;58:693–700. [PubMed: 19066313]
- [14]. Puri P, Mirshahi F, Cheung O, Natarajan R, Maher JW, Kellum JM, et al. Activation and dysregulation of the unfolded protein response in nonalcoholic fatty liver disease. *Gastroenterology* 2008;134:568–576. [PubMed: 18082745]
- [15]. Giménez-Mascarell P, González-Recio I, Fernández-Rodríguez C, Oyenarte I, Müller D, Martínez-Chantar ML, et al. Current structural knowledge on the CNNM family of magnesium transport mediators. *Int J Mol Sci* 2019;20:1135.
- [16]. Daouti S, Li W, Qian H, Huang K-S, Holmgren J, Levin W, et al. A selective phosphatase of regenerating liver phosphatase inhibitor suppresses tumor cell anchorage-independent growth by a novel mechanism involving p130Cas cleavage. *Cancer Res* 2008;68:1162–1169. [PubMed: 18281492]
- [17]. Gulerez I, Funato Y, Wu H, Yang M, Kozlov G, Miki H, et al. Phosphocysteine in the PRL-CNNM pathway mediates magnesium homeostasis. *EMBO Rep* 2016;17:1890–1900. [PubMed: 27856537]
- [18]. Liu M, Yang H, Mao Y. Magnesium and liver disease. *Ann Transl Med* 2019;7:578. [PubMed: 31807559]

- [19]. Chen YS, Kozlov G, Fakih R, Funato Y, Miki H, Gehring K. The cyclic nucleotide-binding homology domain of the integral membrane protein CNNM mediates dimerization and is required for Mg(2+) efflux activity. *J Biol Chem* 2018;293:19998–20007. [PubMed: 30341174]
- [20]. Iruarrizaga-lejarreta M, Varela-Rey M, Fernandez-Ramos D, Martinez-Arranz I, Delgado TC, Simon J, et al. Role of aramchol in steatohepatitis and fibrosis in mice. *Hepatol Commun* 2017;1:911–927. [PubMed: 29159325]
- [21]. Simon J, Nuñez-García M, Fernández-Tussy P, Barbier-Torres L, Fernández-Ramos D, Gómez-Santos B, et al. Targeting hepatic glutaminase 1 ameliorates non-alcoholic steatohepatitis by restoring very-low-density lipoprotein triglyceride assembly. *Cell Metab* 2020;31:605–622. e10. [PubMed: 32084378]
- [22]. Zubiete-Franco I, Fernandez-Tussy P, Barbier-Torres L, Simon J, Fernandez-Ramos D, Lopitz-Otsoa F, et al. Deregulated neddylation in liver fibrosis. *Hepatology* 2017;65:694–709. [PubMed: 28035772]
- [23]. Stephenson K, Kennedy L, Hargrove L, Demieville J, Thomson J, Alpini G, et al. Updates on dietary models of nonalcoholic fatty liver disease: current studies and insights. *Gene Expr* 2018;18:5–17. [PubMed: 29096730]
- [24]. Wolf MJ, Adili A, Piotrowitz K, Abdullah Z, Boege Y, Stemmer K, et al. Metabolic activation of intrahepatic CD8+ T cells and NKT cells causes nonalcoholic steatohepatitis and liver cancer via cross-talk with hepatocytes. *Cancer Cell* 2014;26:549–564. [PubMed: 25314080]
- [25]. Yamazaki S, Miyata H, Funato Y, Fujihara Y, Ikawa M, Miki H. The Mg2+ transporter CNNM4 regulates sperm Ca2+ homeostasis and is essential for reproduction. *J Cell Sci* 2016;129:1940–1949. [PubMed: 27006114]
- [26]. Afzal MS, Pitteloud J-P, Buccella D. Enhanced ratiometric fluorescent indicators for magnesium based on azoles of the heavier chalcogens. *Chem Commun* 2014;50:11358–11361.
- [27]. Rolo AP, Teodoro JS, Palmeira CM. Role of oxidative stress in the pathogenesis of nonalcoholic steatohepatitis. *Free Radic Biol Med* 2012;52:59–69. [PubMed: 22064361]
- [28]. Day CP. From fat to inflammation. *Gastroenterology* 2006;130:207–210. [PubMed: 16401483]
- [29]. Chokshi R, Fruasaha P, Kozak JA. 2-Aminoethy diphenyl borinate (2-APB) inhibits TRPM7 channels through an intracellular acidification mechanism. *Channel* 2012;6:362–369.
- [30]. Zeeshan HMA, Lee GH, Kim H-R, Chae H-J. Endoplasmic reticulum stress and associated ROS. *Int J Mol Sci* 2016;17:327. [PubMed: 26950115]
- [31]. Daw CC, Ramachandran K, Enslow BT, Maity S, Bursic B, Novello MJ, et al. Lactate elicits ER-mitochondrial Mg²⁺ dynamics to integrate cellular metabolism. *Cell* 2020;183:474–489. e17. [PubMed: 33035451]
- [32]. Wan H-X, Hu J-H, Xie R, Yang S-M, Dong H. Important roles of P2Y receptors in the inflammation and cancer of digestive system. *Oncotarget* 2016;7:28736–28747. [PubMed: 26908460]
- [33]. Wu J, Chen S, Liu H, Zhang Z, Ni Z, Chen J, et al. Tunicamycin specifically aggravates ER stress and overcomes chemoresistance in multidrug-resistant gastric cancer cells by inhibiting N-glycosylation. *J Exp Clin Cancer Res* 2018;37:272. [PubMed: 30413206]
- [34]. Malhi H, Kaufman RJ. Endoplasmic reticulum stress in liver disease. *J Hepatol* 2011;54:795–809. [PubMed: 21145844]
- [35]. Park H-W, Park H, Ro S-H, Jang I, Semple IA, Kim DN, et al. Hepatoprotective role of Sestrin2 against chronic ER stress. *Nat Commun* 2014;5:4233. [PubMed: 24947615]
- [36]. Olofsson S, Stillemark-billton P, Asp L. Intracellular assembly of VLDL two major steps in separate cell compartments. *Trends Cardiovasc Med* 2000;10:338–345. [PubMed: 11369260]
- [37]. Millar JS, Cromley DA, Mccoy MG, Rader DJ, Billheimer JT. Determining hepatic triglyceride production in mice: comparison of poloxamer 407 with Triton WR-1339. *J Lipid Res* 2005;46:2023–2028. [PubMed: 15995182]
- [38]. Sirtori CR, Pavanello C, Bertolini S, Sirtori CR, Pavanello C, Bertolini S. Microsomal transfer protein (MTP) inhibition – a novel approach to the treatment of homozygous hypercholesterolemia. *Ann Med* 2014;46:474.
- [39]. Weng Y, Xiao H, Zhang J, Liang X-J, Huang Y. RNAi therapeutic and its innovative biotechnological evolution. *Biotechnol Adv* 2019;37:801–825. [PubMed: 31034960]

- [40]. Altamura S, Schaeper U, Dames S, Löffler K, Eisermann M, Frauendorf C, et al. SLN124, a GalNAc-siRNA conjugate targeting TMPRSS6, efficiently prevents iron overload in hereditary haemochromatosis type 1. *Hemasphere* 2019;3:e301. [PubMed: 31976476]
- [41]. Hirata Y, Funato Y, Takano Y, Miki H. Mg²⁺-dependent interactions of ATP with the cystathionine-beta-synthase (CBS) domains of a magnesium transporter. *J Biol Chem* 2014;289:14731–14739. [PubMed: 24706765]
- [42]. Gordon DA, Wetterau JR, Gregg RE. Microsomal triglyceride transfer protein: a protein complex required for the assembly of lipoprotein particles. *Trends Cell Biol* 1995;5:317–321. [PubMed: 14732096]

Highlights

- CNNM4 acts as a magnesium exporter in the liver. Its upregulation in NASH leads to elevated magnesium levels in serum.
- Liver-specific CNNM4 targeting alleviates steatosis, inflammation, and fibrosis in preclinical NASH models.
- siRNA-mediated CNNM4 downregulation promotes hepatic magnesium accumulation and reduces endoplasmic reticulum stress.
- Silencing CNNM4 enhances microsomal triglyceride transfer protein activity leading to VLDL assembly and secretion.

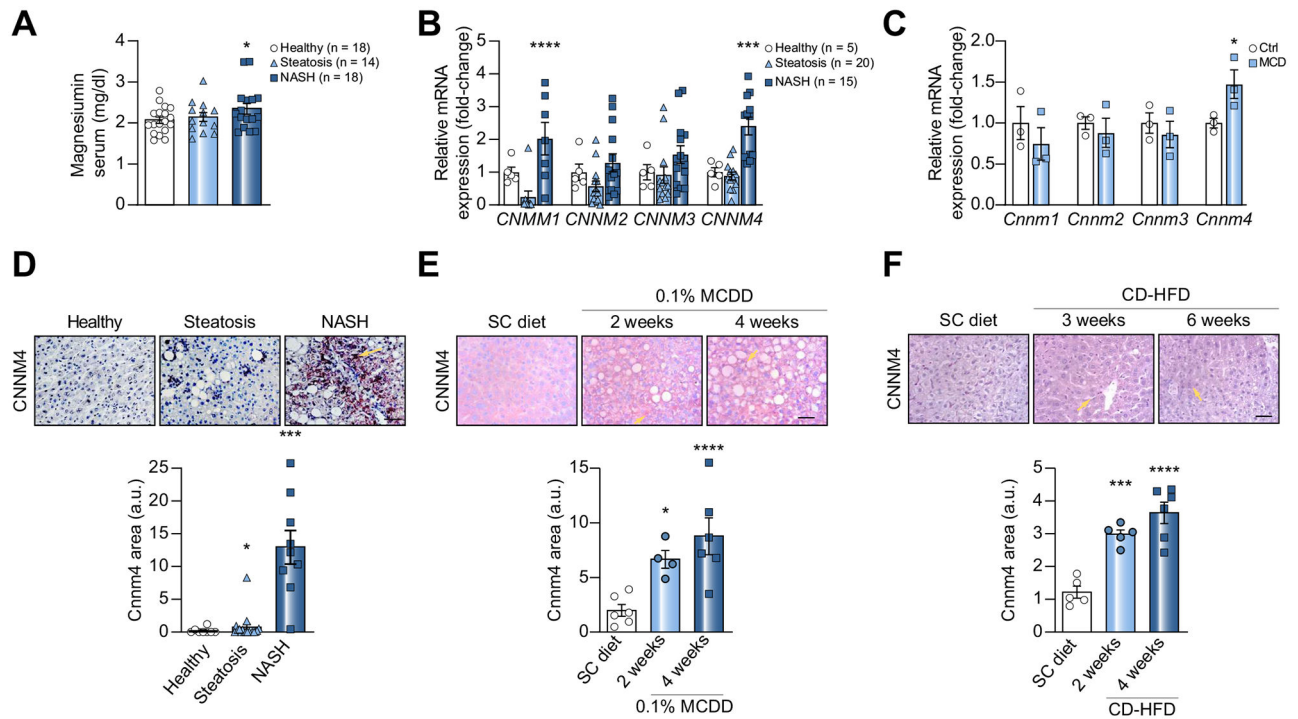


Fig. 1. CNNM4 is overexpressed in NASH patients and preclinical animal models.

(A) Magnesium determination in serum and (B) hepatic levels of *CNNM1-4* mRNA in different cohorts of healthy individuals, patients with steatosis and patients with NASH. (C) Levels of *Cnnm1-4* mRNA in primary hepatocytes stimulated with MCD medium. (D) Liver immunohistochemical staining and quantification for CNNM4 in a cohort of healthy individuals, patients with steatosis and patients with NASH, as well as mice fed (E) a 0.1% MCDD or (F) a CD-HFD. Scale bar corresponds to 100 μ m. * $p < 0.05$, *** $p < 0.001$, and **** $p < 0.0001$ vs. healthy/ctrl/SC diet. CD-HFD, choline-deficient high-fat diet; MCD, methionine and choline deficient; MCDD, MCD diet; NASH, non-alcoholic steatohepatitis; SC diet, regular diet.

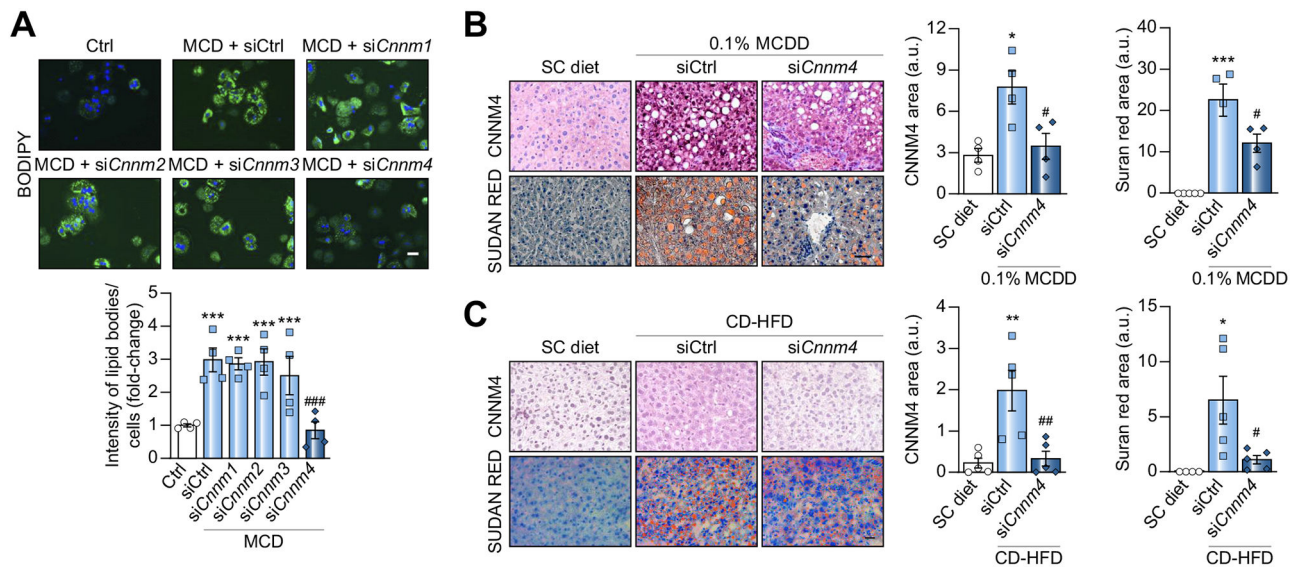


Fig. 2. Targeting CNNM4 reduces lipid accumulation in *in vitro* and *in vivo* NASH models. (A) BODIPY staining micrographs and quantification in primary hepatocytes transfected with siRNA against *Cnm1-4* (si*Cnm1-4*) and stimulated with MCD for 24 h. Micrographs of CNNM4 and Sudan Red staining and respective quantification in mice fed (B) a 0.1% MCD diet (0.1% MCDD) or (C) a CD-HFD, and treated with *Cnm4* siRNA (si*Cnm4*) or an unrelated control (siCtrl). Scale bar corresponds to 50 μ m. * p < 0.05, ** p < 0.01, and *** p < 0.001 vs. Ctrl/SC diet; # p < 0.05, ## p < 0.01, and ### p < 0.001 vs. MCD + siCtrl/0.1% MCDD + siCtrl/CD-HFD + siCtrl. CD-HFD, choline-deficient high-fat diet; MCD, methionine and choline-deficient; NASH, non-alcoholic steatosis; SC diet, regular diet; siRNA, small interfering RNA.

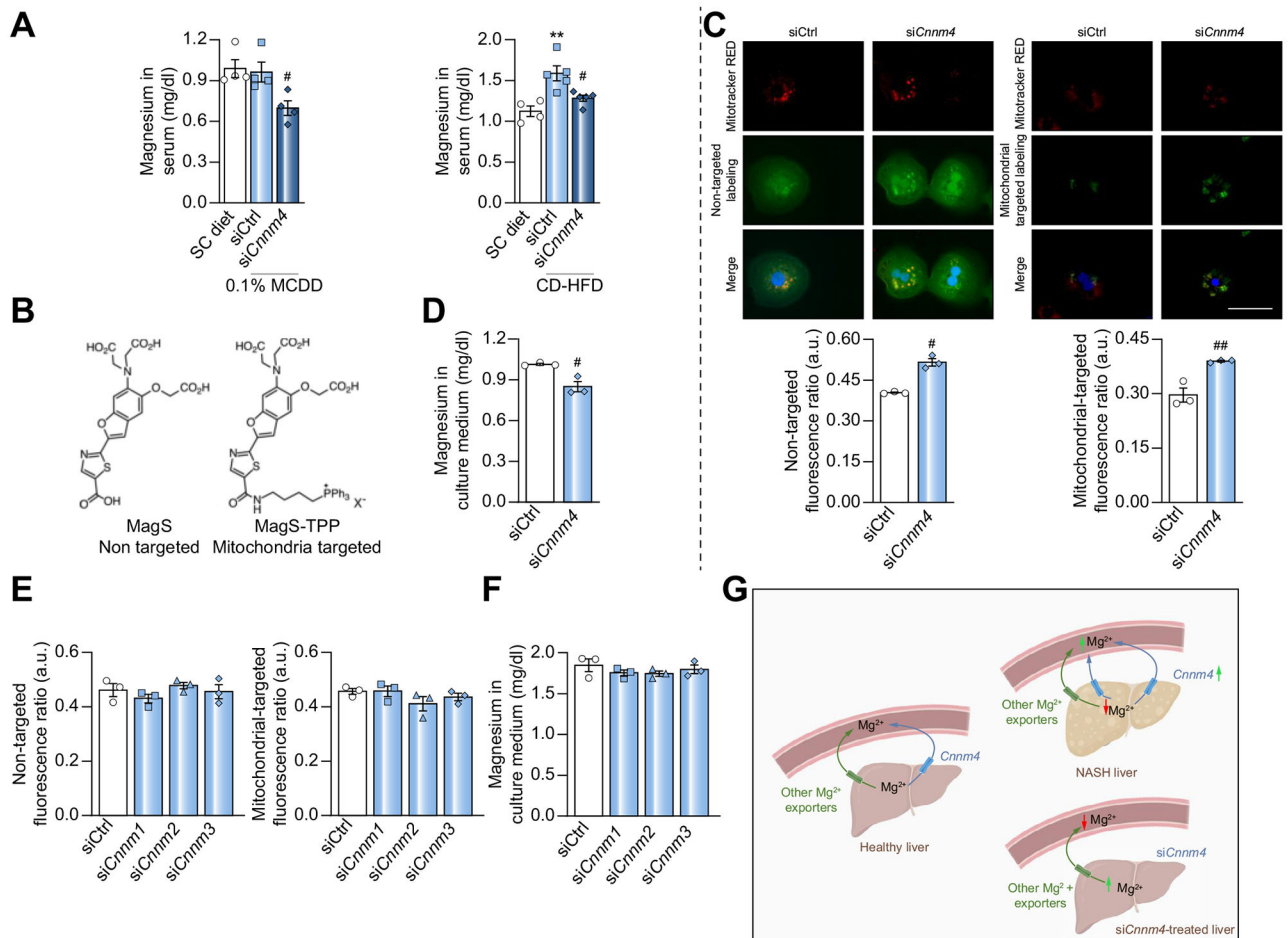


Fig. 3. Magnesium distribution after specific silencing of *Cnnm4*.

(A) Magnesium in serum from mice fed a 0.1% MCDD or CD-HFD with specific *Cnnm4* silencing (si*Cnnm4*) compared with non-treated (siCtrl) mice. (B) Biochemical structure of non-targeted MagS and MagS-TPP probes. (C) Micrographs and relative intracellular magnesium levels and (D) extracellular magnesium levels in primary hepatocytes treated with an siRNA against *Cnnm4* (si*Cnnm4*). Scale bar corresponds to 100 μ m. (E) Intracellular magnesium and (F) extracellular magnesium levels in primary hepatocytes treated with si*Cnnm1-3*. (G) Schematic representation of CNNM4-dependent magnesium fluctuations in liver and in circulation ** $p < 0.01$ vs. SC diet; # $p < 0.05$, and ## $p < 0.01$ vs. 0.1% MCDD + siCtrl/CD-HFD + siCtrl/siCtrl. CD-HFD, choline-deficient high-fat diet; CNNM4, cyclin M4; MagS, magnesium-specific; MagS-TPP, mitochondrion-targeted magnesium-specific; MCDD, methionine and choline deficient diet; siRNA, small-interfering RNA.

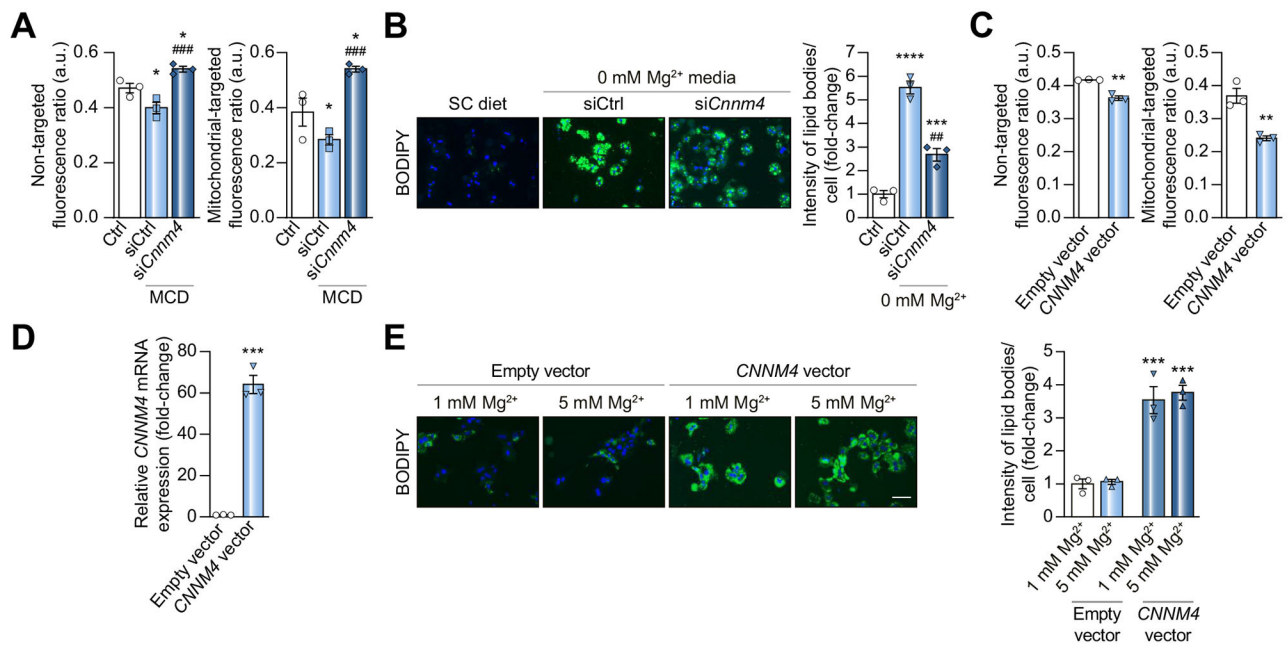


Fig. 4. Modulation of intracellular lipid content by CNNM4.

(A) Relative intracellular magnesium determination by MagS and MagS-TPP staining in primary hepatocytes under MCD stimulation and treated with a *Cnnm4* siRNA (*siCnnm4*). (B) BODIPY staining micrographs and quantification in murine hepatocytes maintained for 24 h under magnesium depletion (0 mM Mg²⁺) and transfected with *siCnnm4*. (C) Relative intracellular magnesium determination and (D) *Cnnm4* mRNA levels in primary hepatocytes transfected for 6 h with an empty or *CNNM4* vector. (E) BODIPY staining micrographs and respective quantification in isolated mouse hepatocytes transfected for 6 h with an empty/*CNNM4* expression vector and stimulated for 24 h with magnesium (5 mM Mg²⁺) vs. a control group (1 mM Mg²⁺). Scale bar corresponds to 100 μm. **p* < 0.05, ***p* < 0.01, ****p* < 0.001, and *****p* < 0.0001 vs. Ctrl/Empty vector; ##*p* < 0.01 and ###*p* < 0.001 vs. MCD + siCtrl/0 mM Mg²⁺ + siCtrl. CD-HFD, choline-deficient high-fat diet; CNNM4, cyclin M4; MagS, magnesium-specific; MagS-TPP, mitochondrion-targeted magnesium-specific; MCD, methionine and choline deficient; siRNA, small interfering RNA.

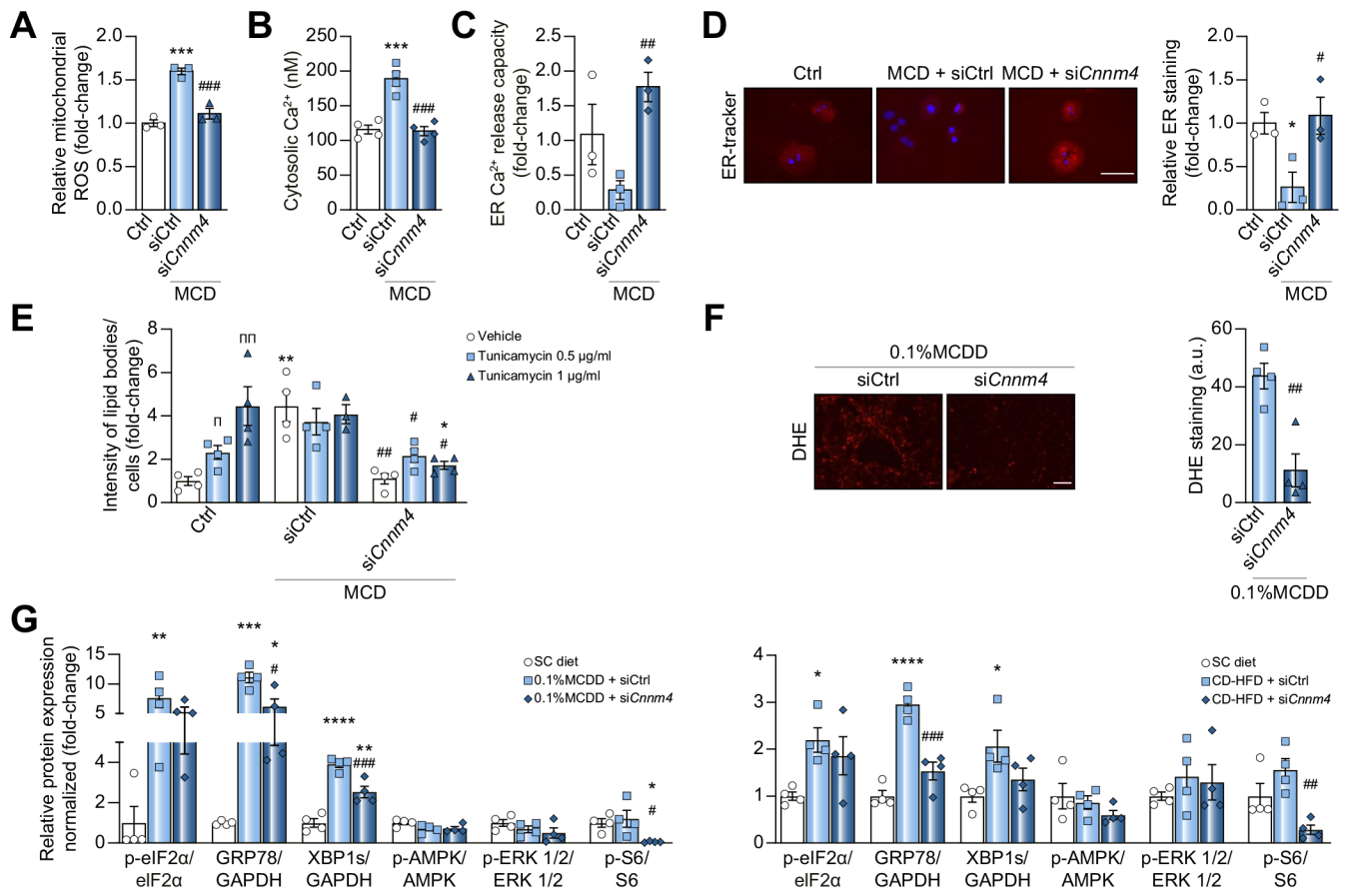


Fig. 5. Specific *Cnnm4* silencing reduces oxidative and ER stress in *in vitro* and *in vivo* NASH models.

(A) Relative mitochondrial ROS levels, (B) cytosolic Ca²⁺ levels, (C) Ca²⁺ release capacity of ER over time and (D) micrographs of ER-tracker red staining and quantification in primary hepatocytes cultured for 24 h in a MCD medium and transfected with a *Cnnm4* (si*Cnnm4*) or control (siCtrl) siRNA. Scale bar corresponds to 100 µm. (E) BODIPY determination in primary hepatocytes treated for 24 h with tunicamycin, MCD, or Ctrl medium and treated with si*Cnnm4* or siCtrl. (F) Representative micrographs (scale bar corresponds to 50 µm) and DHE staining for liver from mice fed a 0.1% MCDD and treated with si*Cnnm4* or siCtrl. (G) Western blot analysis of binding immunoglobulin protein (BIP/GRP78), x-box binding protein 1 isoform s (XBP1s), phospho^{Ser51}-eukaryotic initiation factor 2α (eIF2α), phospho^{Thr172}-AMP dependent protein kinase (AMPK), phospho^{Thr202/Thyr204}-ERK1/2, and phospho^{Ser235/236}-S6 ribosomal protein (S6). Mouse livers from different groups were compared: healthy (SC diet), 0.1% MCDD, or CD-HFD treated with si*Cnnm4* or siCtrl. **p* < 0.05, ***p* < 0.01, ****p* < 0.001, and *****p* < 0.0001 vs. Ctrl/Ctrl + vehicle/SC diet; #*p* < 0.05, ##*p* < 0.01, and ###*p* < 0.001 vs. MCD + siCtrl/0.1% MCDD + siCtrl/MCD + vehicle + siCtrl/CDHFD + siCtrl; π*p* < 0.05 and ππ*p* < 0.01 for vehicle vs. tunicamycin. CD-HFD, choline-deficient high-fat diet; CNNM4, cyclin M4; DHE, dihydroxyethyl; ER, endoplasmic reticulum; MCD, methionine and choline deficient; MCDD, MCD diet; NASH, non-alcoholic steatohepatitis; ROS, reactive oxygen species; SC, regular diet; siRNA, small interfering RNA.

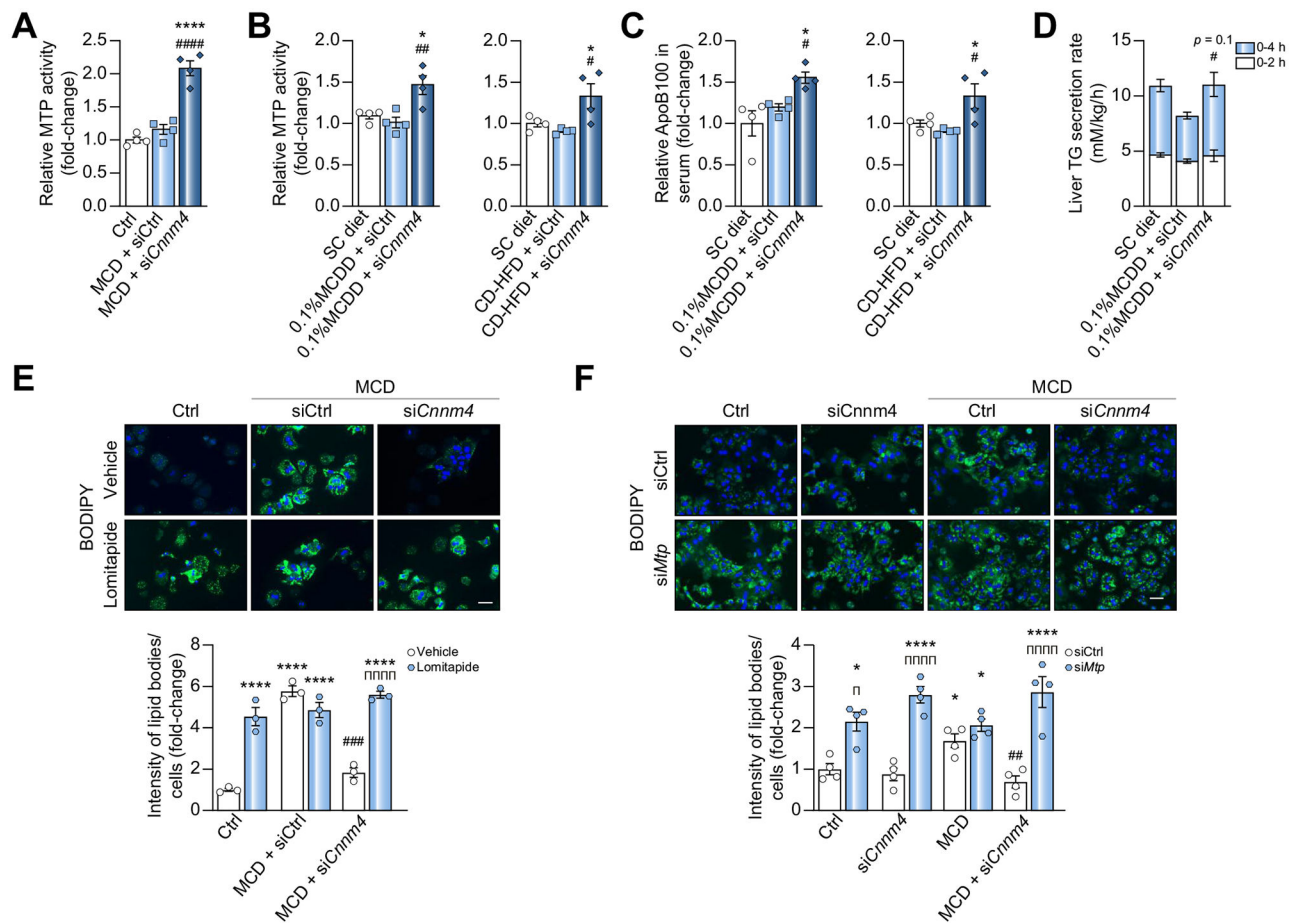


Fig. 6. Inhibition of CNNM4 expression promotes lipid export by activating MTP activity. (A) Relative MTP activity in primary hepatocytes cultured for 24 h in a MCD medium and transfected with a *Cnnm4* siRNA (si*Cnnm4*) or unrelated control (siCtrl). (B) Relative MTP activity in livers from mice fed a 0.1% MCDD or a CD-HFD and treated with si*Cnnm4* or siCtrl. (C) Relative apolipoprotein B100 (APOB100) levels in sera from mice fed a 0.1% MCDD or CD-HFD and treated with si*Cnnm4* or siCtrl. (D) Liver TG secretion rate in mice fed a 0.1% MCDD, treated with si*Cnnm4* or siCtrl and after poloxamer P407 administration. BODIPY staining micrographs and quantification of primary hepatocytes cultured under MCD and treated with siCtrl or si*Cnnm4* and (E) a vehicle (DMSO) or 600 nM lomitapide for 24 h or (F) an siRNA against *Mtp* (si*Mtp*). Scale bar corresponds to 100 μ m. * p < 0.05 and **** p < 0.0001 vs. SC diet/Ctrl + vehicle/Ctrl + siCtrl; # p < 0.05, ## p < 0.01, ### p < 0.001, and #### p < 0.0001 vs. 0.1% MCDD + siCtrl/CD-HFD + siCtrl/MCD + vehicle + siCtrl/MCD + siCtrl; π p < 0.05 and $\pi\pi\pi\pi$ p < 0.0001 for vehicle/siCtrl vs. lomitapide/si*Mtp*. CD-HFD, choline-deficient high-fat diet; MCD, methionine and choline deficient; MCDD, MCD diet; MTP, microsomal triglyceride transfer protein; SC, regular diet; siRNA, small interfering RNA; TG, triacylglyceride.

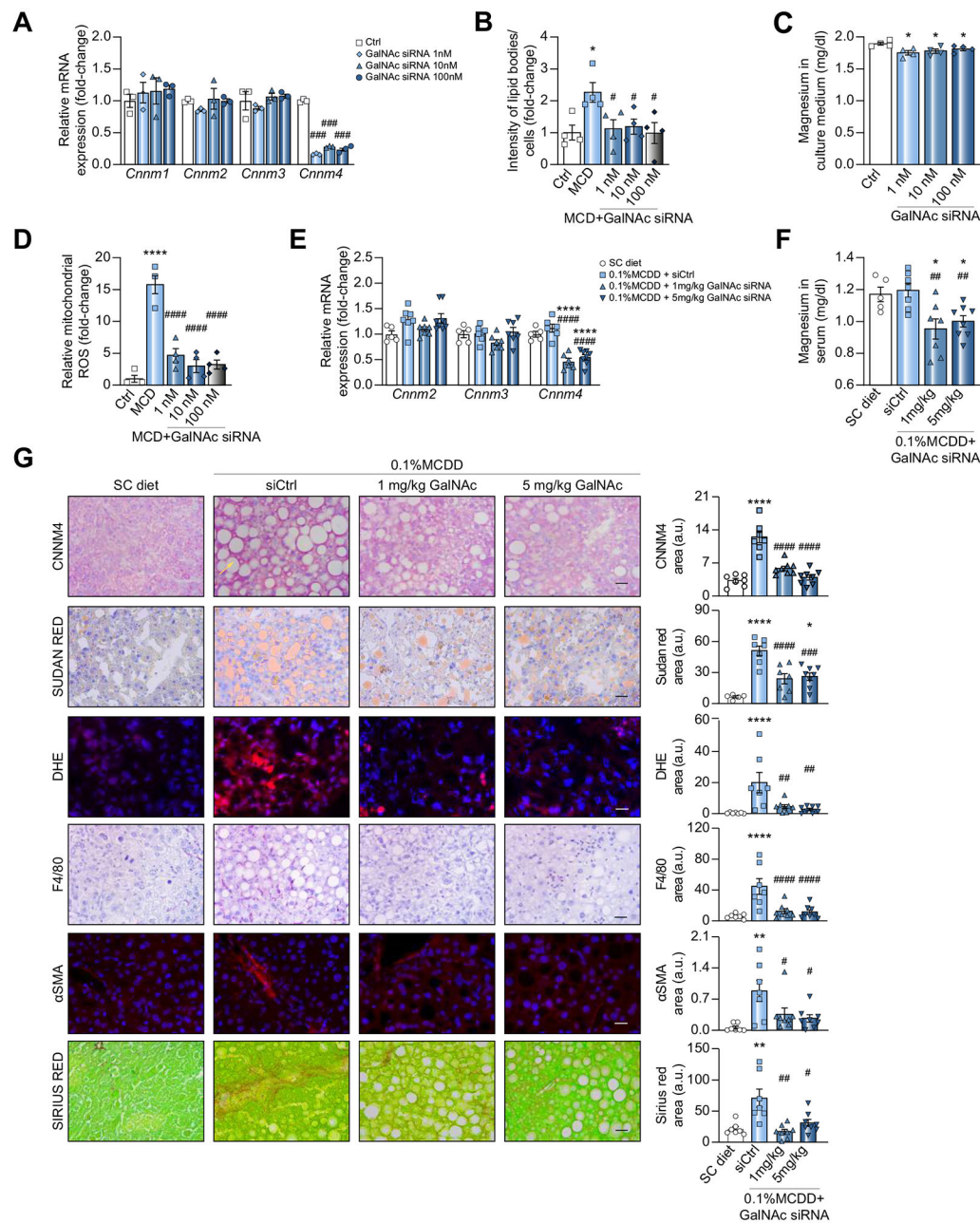


Fig. 7. Inhibition of CNNM4 expression by GalNAc-siRNA conjugate reduces NASH in preclinical models

Levels of (A) *Cnnm1-3* mRNA and (C) magnesium in extracellular medium from primary hepatocytes treated overnight with a GalNAc-conjugated siRNA against *Cnnm4* (GalNAc siRNA) and a MCD medium. Relative determination of (B) lipid accumulation and (D) mitochondrial ROS production in primary hepatocytes treated with an MCD and Ctrl or GalNAc siRNA. Relative levels of (E) *Cnnm1-4* mRNA and (F) Mg^{2+} in serum, and (G) histological characterisation of CNNM4, lipids (Sudan Red), inflammation (F4/80 and DHE) and fibrosis (α SMA and Sirius Red) in livers from mice fed a 0.1% MCDD and treated with siCtrl or GalNAc siRNA. * $p < 0.05$, ** $p < 0.01$, and **** $p < 0.0001$ vs. Ctrl/SC

diet; $^{\#}p < 0.05$, $^{\#\#}p < 0.01$, $^{\#\#\#}p < 0.001$, and $^{\#\#\#\#}p < 0.01$ vs. MCD + siCtrl/0.1% MCDD + siCtrl. CD-HFD, choline-deficient high-fat diet; CNNM4, cyclin M4; DHE, dihydroxyethyl; GalNAc, N-acetylgalactosamine; MCD, methionine and choline deficient; MCDD, MCD diet; NASH, non-alcoholic steatohepatitis; ROS, reactive oxygen species; siRNA, small interfering RNA.

Author Manuscript

Author Manuscript

Author Manuscript

Author Manuscript